We are IntechOpen, the world's leading publisher of Open Access books Built by scientists, for scientists

4,800
Open access books available

122,000
International authors and editors

135M
Downloads

Our authors are among the

154
Countries delivered to

TOP 1%
most cited scientists

12.2%
Contributors from top 500 universities

CLARIVATE ANALYTICS BOOK CITATION INDEX INDEXED

WEB OF SCIENCE™

Selection of our books indexed in the Book Citation Index in Web of Science™ Core Collection (BKCI)

Interested in publishing with us?
Contact book.department@intechopen.com

Numbers displayed above are based on latest data collected.
For more information visit www.intechopen.com

7

Semi-Empirical Modelling and Management of Flotation Deinking Banks by Process Simulation

Davide Beneventi[1], Olivier Baudouin[2] and Patrice Nortier[1]
[1]*Laboratoire de Génie des Procédés Papetiers (LGP2), UMR CNRS 5518, Grenoble INP-Pagora - 461, rue de la Papeterie - 38402 Saint-Martin-d'Hères,*
[2]*ProSim SA, Stratège Bâtiment A, BP 27210, F-31672 Labege Cedex, France*

1. Introduction

Energy use rationalization and the substitution of fossil with renewable hydrocarbon sources can be considered as some of the most challenging objectives for the sustainable development of industrial activities. In this context, the environmental impact of recovered papers deinking is questioned (Byström & Lönnstedt, 2000) and the use of recovered cellulose fibres for the production of bio-fuel and carbohydrate-based chemicals (Hunter, 2007; Sjoede et al., 2007) is becoming a possible alternative to papermaking. Though there is still room for making radical changes in deinking technology and/or in intensifying the number of unit operations (Julien Saint Amand, 1999; Kemper, 1999), the current state of the paper industry dictates that most effort be devoted to reduce cost by optimizing the design of flotation units (Chaiarrekij et al., 2000; Hernandez et al., 2003), multistage banks (Dreyer et al., 2008; Cho et al., 2009; Beneventi et al., 2009) and the use of deinking additives (Johansson & Strom, 1998; Theander & Pugh, 2004). Thereafter, the improvement of the flotation deinking operation towards lower energy consumption and higher separation selectivity appears to be necessary for a sustainable use of recovered fibres in papermaking.
Nevertheless, over complex physical laws governing physico-chemical interactions and mass transport phenomena in aerated pulp slurries (Bloom & Heindel, 2003; Bloom, 2006), the variable composition and sorting difficulties of raw materials (Carré & Magnin, 2003; Tatzer et al., 2005) hinder the use of a mechanistic approach for the simulation of the flotation deinking process. At this time, the use of model mass transfer equations and the experimental determination of the corresponding transport coefficients is the most widely used method for the accurate simulation of flotation deinking mills (Labidi et al., 2007; Miranda et al., 2009; Cho et al., 2009).
Solving the mass balance equations in flotation deinking and generally in papermaking systems with several recycling loops and constraints is not straightforward: this requires explicit treatment of the convergence by a robust algorithm and thus computer-aided process simulation appears as one of the most attractive tools for this purpose (Ruiz et al., 2003; Blanco et al., 2006; Beneventi et al., 2009). Process simulation software are widely used in papermaking (Dahlquist, 2008) for process improvement and to define new control strategies. However, paper deinking mills have been involved in this process rationalization

Source: Process Management, Book edited by: Mária Pomffyová,
ISBN 978-953-307-085-8, pp. 338, April 2010, INTECH, Croatia, downloaded from SCIYO.COM

effort only recently and the full potential of process simulation for the optimization and management of flotation deinking lines remains underexploited.

This chapter describes the four stages that have been necessary for the development of a flotation deinking simulation module based on a semi-empirical approach, i.e.:

- the identification of transport mechanisms and their corresponding mass transfer equations;
- the validation of model equations on a laboratory-scale flotation cell;
- the correlation of mass transfer coefficients with the addition of chemical additives in the pulp slurry;
- the implementation of model equations on a commercial process simulation platform, the simulation of industrial flotation deinking banks and the comparison of simulation results with mill data.

After the validation of the simulation methodology, deinking lines with different configurations are simulated in order to evaluate the impact of line design on process efficiency and specific energy consumption. As a step in this direction, single-stage with mixed tank/column cells, two-stage and three-stage configurations are evaluated and the total number of flotation units in each stage and their interconnection are used as main variables. Explicit correlations between ink removal efficiency, selectivity, energy consumption and line design are developed for each configuration showing that the performance of conventional flotation deinking banks can be improved by optimizing process design and by implementing mixed tank/column technologies in the same deinking line.

2. Particle transport mechanisms

Particle transport in flotation deinking cells can be modelled using semi-empirical equations accounting for four main transport phenomena, namely, hydrophobic particle flotation, entrainment and particle/water drainage in the froth (Beneventi et al., 2006).

2.1 Flotation

In flotation deinking system, the gas and the solid phases are finely dispersed in water as bubbles and particles with size ranging between ~0.2 – 2 mm and ~10 – 100 μm, respectively. The collision between bubbles and hydrophobic particles can induce the formation of stable bubble/particle aggregates which are conveyed towards the surface of the liquid by convective forces (Fig. 1a). Similarly, lipophilic molecules adsorbed at the air/water interface are removed from the pulp slurry by air bubbles (Fig. 1b). The rate of removal of hydrophobic materials by adsorption/adhesion at the surface of air bubbles, r_n^f, can be described by the typical first order kinetic equation

$$r_n^f = k_n \cdot c_n \tag{1}$$

where c_n is the concentration of a specific type of particle (namely, ink, ash, organic fine elements and cellulose fibres) and k_n its corresponding flotation rate constant,

$$k_n = \frac{K_n \cdot Q_g^{\alpha}}{S} \tag{2}$$

Q_g is the gas flow, α an empirical parameter, S is the cross sectional area of the flotation cell and K_n is an experimentally determined parameter including particle/bubble collision dynamics and physicochemical factors affecting particle adhesion to the bubble surface.

2.2 Entrainment

During the rising motion of an air bubble in water, a low pressure area forms in the wake of the bubble inducing the formation of eddies with size and stability depending on bubble size and rising velocity. Both hydrophobic and hydrophilic small particles can remain trapped in eddy streamlines (Fig. 1c) and they can be subsequently entrained by the rising motion of air bubbles.

Particles and solutes entrainment is correlated to their concentration in the pulp slurry and to the water upward flow in the froth (Zheng et al., 2005).

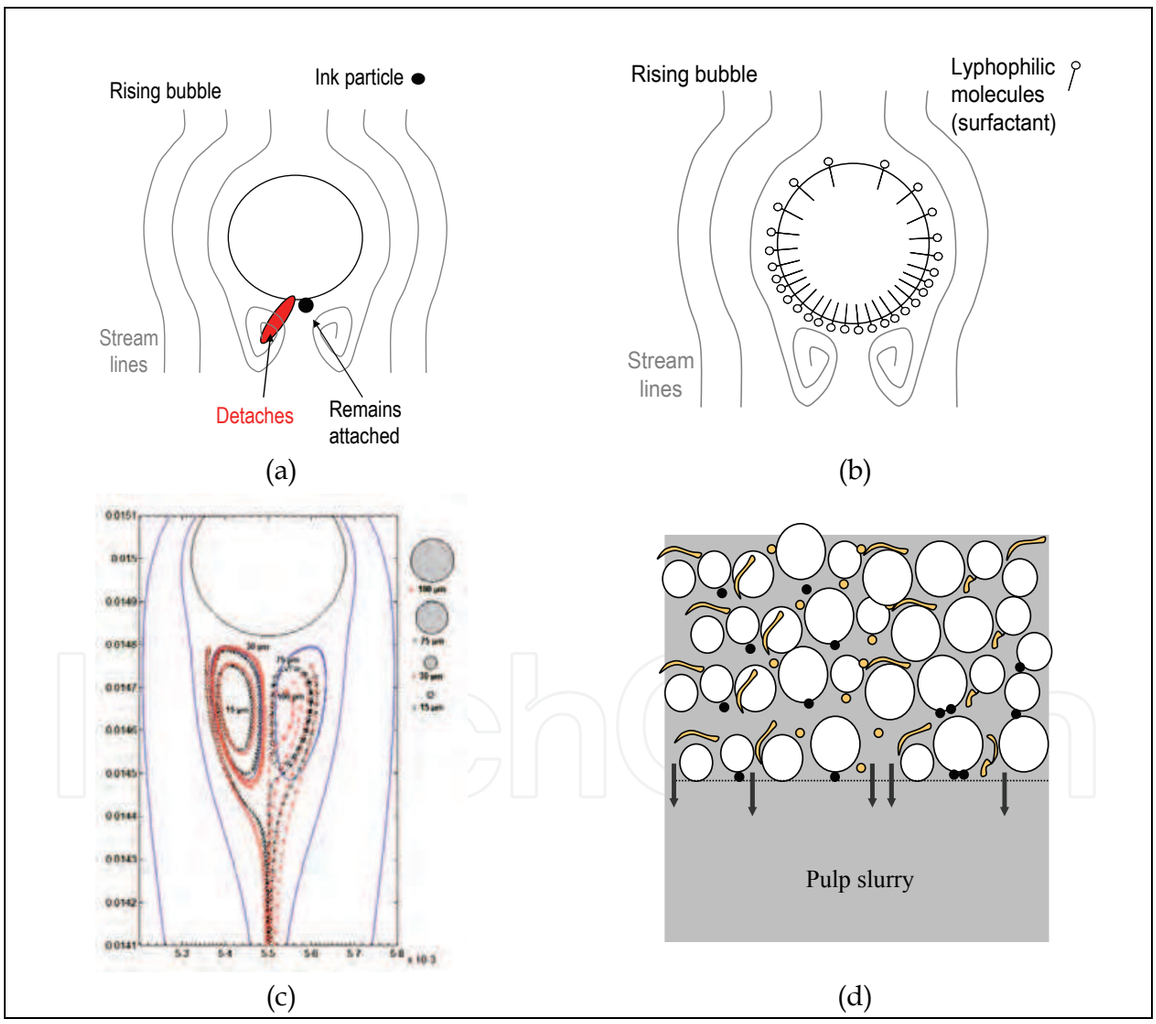

Fig. 1. Scheme of transport mechanisms acting during the flotation deinking process. (a) Particle attachment and flotation, (b) liphopilic molecules adsorption, (c) influence of size on the path of cellulose particle in the wake of an air bubble (Beneventi et al. 2007), (d) water and particle drainage in the froth.

The rate of removal due to entrainment, r_n^e, can be modelled by the equation:

$$r_n^e = \frac{\phi \cdot Q_f^0}{V} c_n \tag{3}$$

where $\phi = c_{0f}/c_n$ is the entrainment coefficient, c_{0f} is particle concentration at the pulp/froth interface, Q_f^0 is the water upward flow in the froth in the absence of drainage and V is the pulp volume in the flotation cell.
The total rate of removal due to both flotation and entrainment is given by the sum of the two contributions, i.e. $r_n^{up} = r_n^f + r_n^e$.

2.3 Water and particle drainage in the froth

At the surface of the aerated pulp slurry, a froth phase is formed with water films dividing neighbouring bubbles and solid particles either dispersed in the liquid phase or attached to the surface of froth bubbles (Fig. 1d). Despite the complex dynamics of froth systems (Neethilng & Cilliers, 2002), water and particle drainage induced by gravitational forces can be considered as the two main phenomena governing mass transfers in the froth.
The water drainage through the froth, described using the water hold-up in the froth (ε), and the froth retention time (FRT) in the flotation cell were taken as main parameters:

$$\varepsilon = \frac{Q_f}{Q_f + Q_g}, \tag{4}$$

$$FRT = \frac{h}{J_g + J_f} \tag{5}$$

where Q_g and Q_f are the gas and the froth reject flows, h is the froth thickness and J_g, J_f are the gas and water superficial velocities in the froth. In flotation froths, the decrease of water hold-up versus time, is well described by an exponential decay (Gorain et al., 1998; Zheng et al., 2006)

$$\frac{\varepsilon}{\varepsilon_0} = e^{-L_d \cdot FRT} \tag{6}$$

where ε_0 is the water volume fraction at the froth/pulp interface and L_d is the water drainage rate constant.
By analogy with particle entrainment in the aerated pulp slurry, the rate of the entrainment of particles/solutes dispersed in the froth by the water drainage stream, r_n^{down}, is given by the equation

$$r_n^{down} = \delta \cdot c_{nf} \cdot Q_d / V \tag{7}$$

where $\delta = c_d/c_{nf}$ is the particle drainage coefficient, c_{nf} and c_d are particle concentrations in the froth and in the water drainage stream, respectively and Q_d is the water drainage flow.
In order to close-up Eqs. (1-7), perfect mixing is assumed in the lower part and two counter-current piston flows in the upper part (upward flow for the froth and downward flow for water drainage).

3. Validation of model equations at the laboratory scale

Mechanisms described by Eqs. (1-7) are extensively used in minerals flotation for the simulation of industrial processes. Nevertheless, due to the intrinsic difference between the composition and the rheological behaviour of minerals and recovered papers slurries, the use of Eqs. (1-7) for the simulation of industrial flotation deinking processes is not straightforward and model validation on a pilot flotation cell appears a necessary step.

3.1 Flotation cell set-up and flotation conditions

To run pilot tests, a 19 cm diameter and 130 cm height flotation column was assembled (Fig. 2). The flotation column has two main regions: a collection region, where the pulp slurry is in contact with gas bubbles, and a ~15 cm height aeration region, where the pulp is re-circulated in tangential Venturi aerators where the gas flow is regulated by using a mass flow meter. The froth generated at the top of the flotation column is removed by using an adjustable reverse funnel connected to a vacuum pump. The pulp level in the cell and the froth retention time before removal can be modified by adjusting the position of the overflow system and of the reverse funnel, respectively.

The retention time distribution obtained in the absence and in the presence of cellulose fibres (Fig. 3) shows that, whatever the liquid volume in the cell and the feed flow, the flotation cell can be described as a continuous stirred tank reactor (CSTR).

Flotation experiments were performed using a conventional fatty acid chemical system in order to test independently the contribution of air flow, pulp feed flow, pulp hydraulic retention time in the cell and froth retention time on the ink removal efficiency and the flotation yield. Experimental conditions are summarized in Table 1.

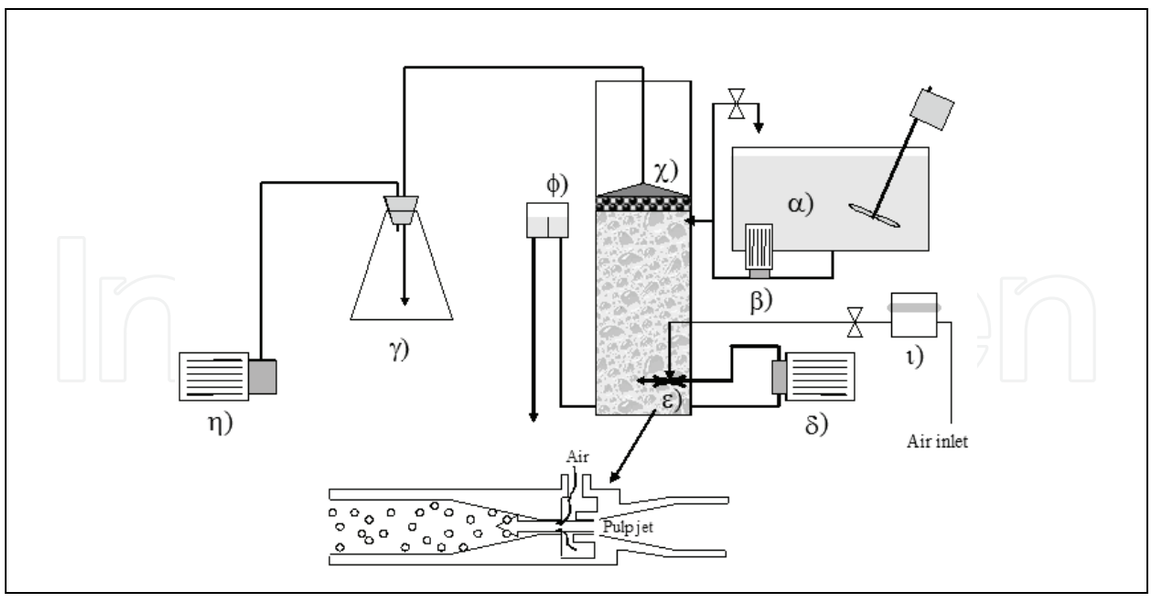

Fig. 2. Schematic representation of the flotation column used in this study. α) Pulp storage chest. β) Volumetric pump. χ) Adjustable froth removal device. δ) Volumetric pump to supply gas injectors. ε) Venturi-type air injectors. ϕ) Flotation cell outlet with adjustable overflow system. γ) Froth collection vessel. η) Vacuum pump. ι) Mass flow meter.

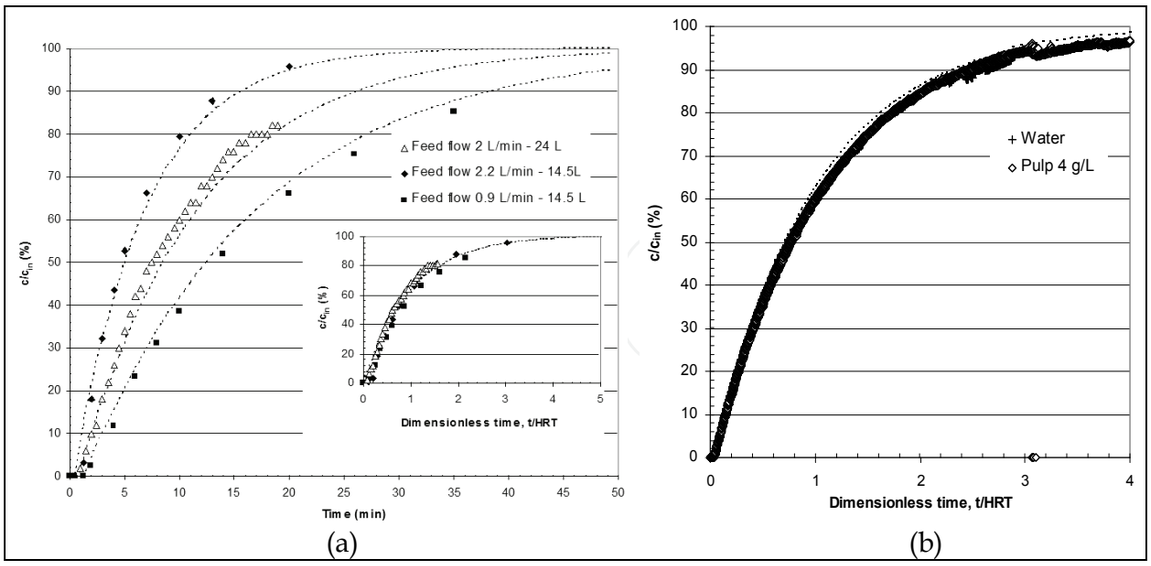

Fig. 3. Mixing conditions in the flotation column. Reactor response to a step type increase in the tracer concentration. (a) Effect of the feed flow and cell volume in presence of water (b) Effect of cellulose fibres. Dotted lines represent the CSTR response.

Cell Volume V (L)	Pulp flow Q_{in} (L/min)	Air flow Q_g (L/min)	Froth removal thickness h (cm)	HRT V/Q_{in} (min)	Air ratio Q_g/Q_{in} (%)
14.5	2	4	3 - 1.5 - 4 - 8	7.2	200
14.5	2	6	3 - 1.5 - 4 - 8	7.2	200
14.5	2	8	3 - 1.5 - 4 - 8	7.2	200
14.5	3.5	4	3 - 1.5 - 4 - 8	4.1	114
14.5	4.5	4	3 - 1.5 - 4 - 8	3.2	89
14.5	2.5	5	3 - 1.5 - 5 - 8	5.8	200
19.5	2.5	5	3 - 1.5 - 5 - 8	7.8	200
24	2.5	5	3 - 1.5 - 5 - 8	9.6	200

Table 1. Experimental conditions used to run flotation trials. The cross sectional area of the flotation column had a constant value, S = 283 cm².

3.2 Interpretation of experimental results with model equations

3.2.1 Water removal

Froth flows measured during flotation experiments were fitted by using Eqs. (5, 6) and the water volume fraction in the top froth layer before removal was plotted as a function of the froth retention time in the cell. Fig. 4 shows that the water fraction in the froth had an exponential decay with increasing retention time and that Eq. (6) fitted with good accuracy experimental data. The absence of froth recovery when the retention time was higher than 30 s indicates that, when the water fraction was lower than ~0.02, gas bubbles collapsed in the reverse funnel and froth recovery was no longer possible. The decrease of froth processability in the vacuum system was attributed to the destabilization of froth liquid film and to the typical increase in froth viscosity (Shi & Zheng, 2003) when increasing FRT.

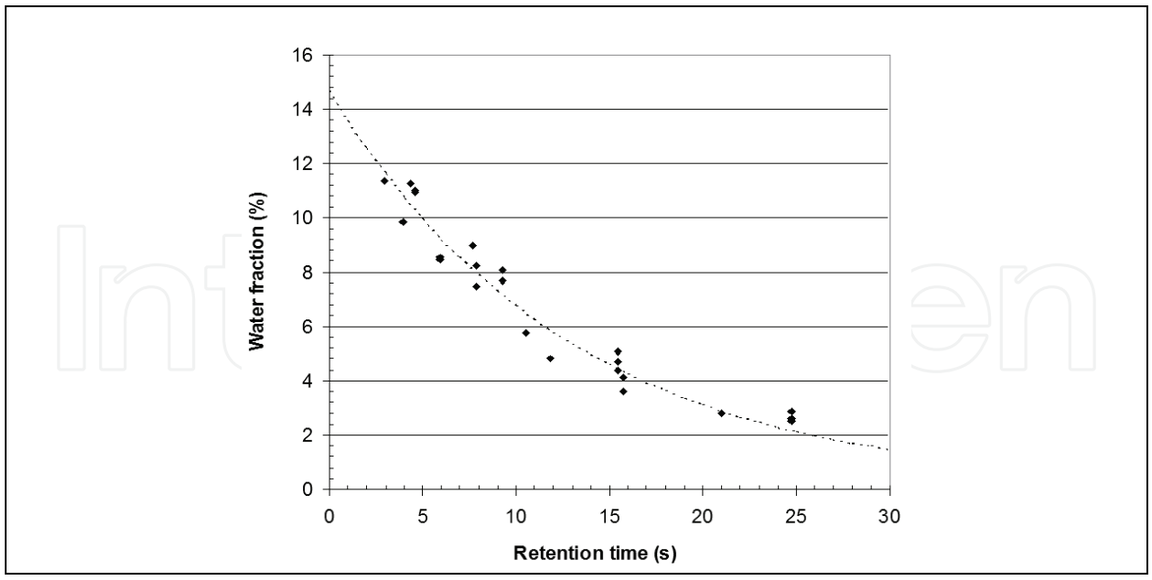

Fig. 4. Water volume fraction in the froth removed by the vacuum device (all tested conditions) plotted as a function of the froth retention time in the cell.

The frothing behaviour of the pulp slurry was therefore described by Eq. 6, with ε_o = 0.15 and L_d = 4.44 min^{-1}.

3.2.2 Ink removal

The variation of the ink concentration during the flotation transitory and steady states and with froth removal at different heights, were obtained by mass balance from Eqs. (2-7) and the models of reactors. In order to limit the number of free variables in the equation system, the entrainment coefficient of ink particles was assumed similar to that of silica particles with same size (Machaar & Dobby, 1992), namely ~0.2. As expected from Eq. (2), the increase in the gas flow gave a corresponding increase in the ink flotation rate constant which fairly deviated from a linear correlation, i.e. $k_{ink} = 0.15\ Q_g^{0.73}$ (k in min^{-1}, Q_g in L/min). The ink drainage coefficient given by model equations was δ_{ink} = 0.30, thus reflecting the limited drainage of ink particles through the froth and the low variation of ink concentration in the pulp when the froth removal height was increased (Fig. 5a). Flotation rate constants and ink drainage coefficient obtained by fitting experimental data were used to predict the contribution of cell volume and froth removal height on the residual ink concentration in the pulp. Calculated ink removal efficiencies matched with experimental values (Fig. 5b).

3.3.3 Fibres removal

This approach was repeated for fibres, fines and ashes. Since cellulose fibres are hydrophilic particles with large-un-floatable size (~1.5x0.1 mm), only entrainment and drainage were assumed to govern their transport during flotation.

Fitting of experimental data gave an entrainment coefficient extremely high for this class of large particles: ϕ_{fibres} = 0.30, and a drainage coefficient of δ_{fibres} = 0.80. The relevant contribution of entrainment was associated with the natural tendency of cellulose fibres to generate large flocks with small gas bubbles trapped in.

3.3.4 Fines and ash removal

Fines and ashes displayed an intermediate behaviour between ink and fibres. Fitting of experimental data gave low flotation rate constants proportional to the gas flow, $k_{fines} = 0.018\ Q_g$ for fines and $k_{ash} = 0.021\ Q_g$ for ash (k in min^{-1}, Q_g in L/min).

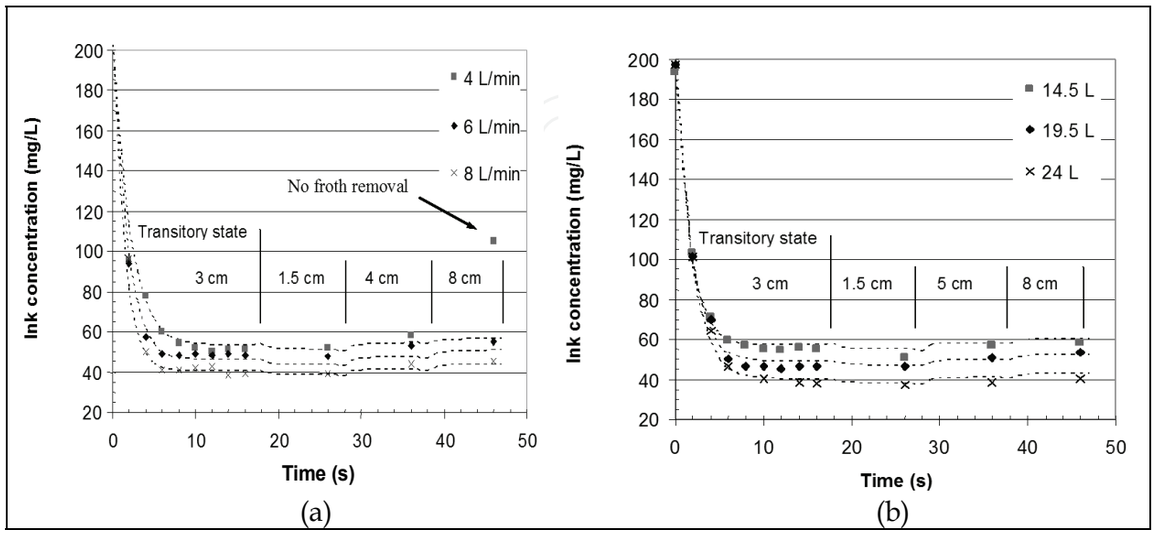

Fig. 5. Variation of ink concentration plotted as a function of the flotation time and of the froth removal height. (a) Influence of gas flow on residual ink concentration, pulp flow Q_{in} = 2 L/min, cell volume V = 14.5 L. Dotted lines represent experimental data fitting with model equations. (b) Influence of cell volume on residual ink concentration, pulp flow Q_{in} = 2.5 L/min, gas flow Q_g = 5 L/min. Dotted lines represent trends obtained from model calculations.

Like ink particles, entrainment coefficients for fines and ash were assumed similar to that of silica particles with similar size, namely ϕ_{fines} = 0.25 and ϕ_{ash} = 0.45 and, as expected for poorly floatable particles, drainage coefficients had high values, namely δ_{fines} = 0.85 and δ_{ash} = 0.8.

Present results show that model equations derived from the minerals flotation field allowed modelling the flotation deinking of recovered papers when using a conventional-fatty acid chemical system. The contribution of pulp flow, cell volume, viz. HRT, and froth removal height on ink removal and yield was predicted with good accuracy. However, chemical variables (such as the presence of surfactants), which can strongly affect the flotation deinking process, were not accounted in the model. As a step in this direction, the contribution of a model non-ionic surfactant on particle and water transport was investigated.

4. Correlation of transport coefficients with surfactant addition

Recovered papers may release in process waters a wide variety of dissolved and colloidal substances (Brun et al., 2003; Pirttinen & Stenius, 1998) which limit the use of conventional analytical techniques for the dosage of non-ionic surfactants. In order to avoid using over complex purification and analysis procedures, the surfactant concentration in the pulp slurry can be estimated using an indirect method based on the measurement of surface

tension by maximum bubble pressure (Pugh, 2001; Comley et al., 2002). Thereafter, in the presence of a reference surfactant (in this study, an alkyl phenol ethoxylate, NP 20EO, added at the inlet of the flotation cell) it becomes possible to quantify the effect of surfactant concentration on particle, water and surfactant molecules transport during the flotation process and to establish direct cross correlations between surfactant concentration and transport coefficients.

4.1 Surfactant removal

The removal of surfactant molecules from the pulp slurry during flotation is strongly affected by surfactant concentration and by the froth removal thickness (Fig. 6a). Indeed, the increase in NP 20EO concentration boosted surfactant removal and decreased the impact of the froth removal thickness on the residual surfactant in the floated pulp. Surfactant removal rates and drainage coefficients (Fig. 6b) obtained by fitting experimental data with Eqs. (1-7), show that the removal rate constant increased with the equivalent concentration, while the drainage coefficient decreased. This trend was interpreted as reflecting the contribution of the initial surfactant concentration on bubble size and on froth stability: a decrease in bubble coalescence/burst in the aerated pulp and in the froth leads to an increase in the surfactant removal rate and a decrease in the drainage rate, respectively.

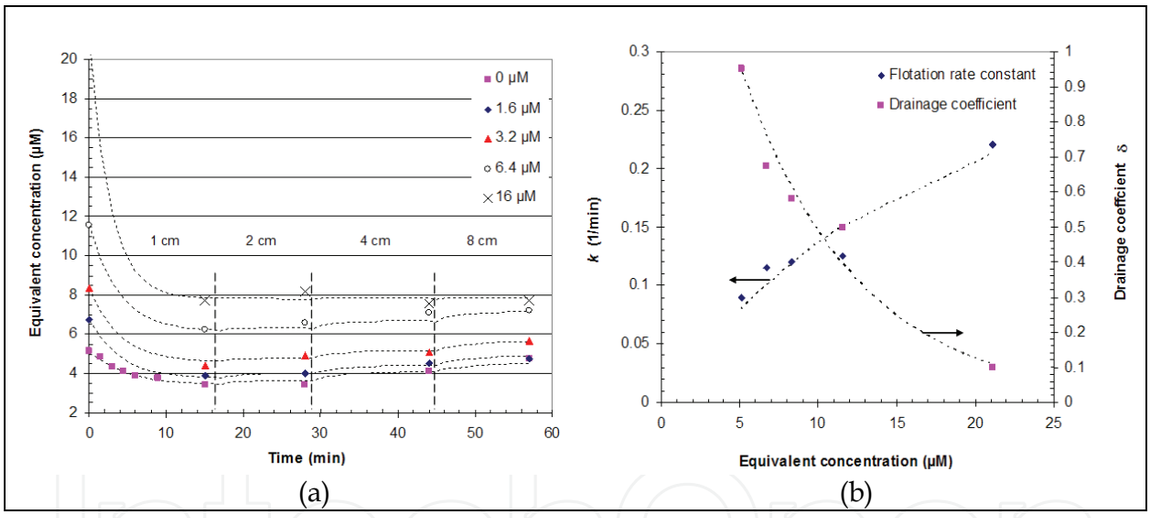

Fig. 6. Surfactant removal from the pulp slurry during flotation. (a) Decrease in the surfactant equivalent concentration in the pulp slurry during flotation plotted as a function of the froth removal thickness and of NP 20EO concentration (dotted lines represent data fitting with Eqs. (1-7). (b) Surfactant removal rate constant and drainage coefficient obtained from the interpolation of experimental data with model equations.

4.2 Gas and water hold-up

Fig. 7 shows that the rise in the surfactant flotation rate constant (Fig. 6b) can be ascribed to an increase in the gas hold-up with the surfactant concentration. This trend is due to the bubble stabilization induced by the adsorption of surfactant molecules on the bubble surface and the ensuing stabilization of liquid films formed between colliding bubbles (Danov et al., 1999; Valkovska et al., 2000). The water hold-up in the froth calculated from water recovery data and Eqs. (5, 6) shows an exponential decay (Fig. 8a) and the water hold-up at the

pulp/froth interface, ε_0, increases with the surfactant concentration, whereas the water drainage coefficient, L_d, decreases (Fig. 8b). This trend reflects the NP 20EO contribution in i) decreasing bubble size in the aerated pulp, ii) stabilizing liquid films between froth bubbles and iii) preventing bubble burst in the froth.

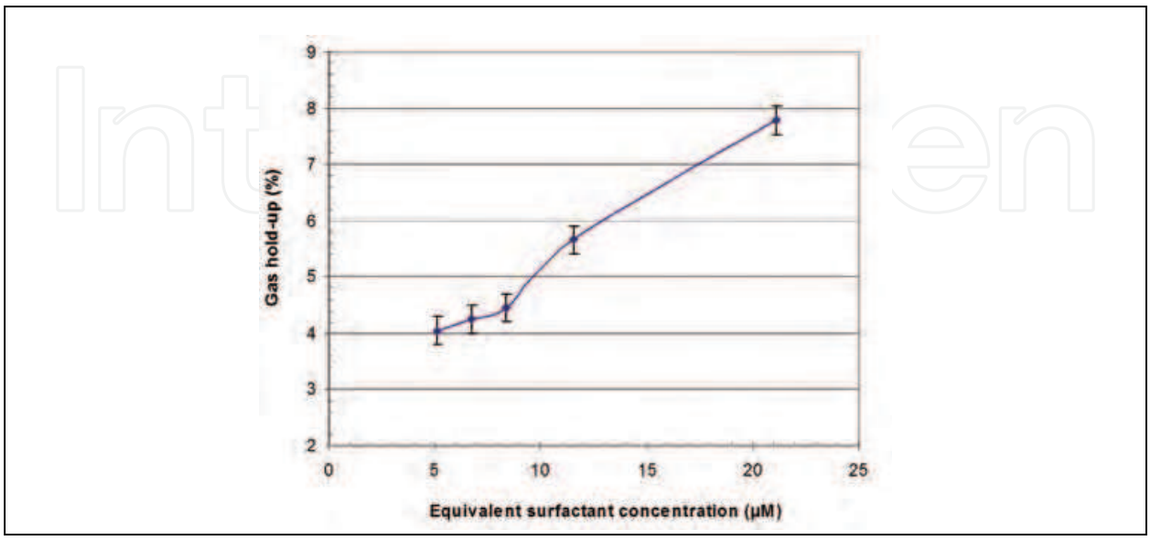

Fig. 7. Effect of the model non-ionic surfactant (NP 20EO) on gas hold-up. Air flow 2 L/min.

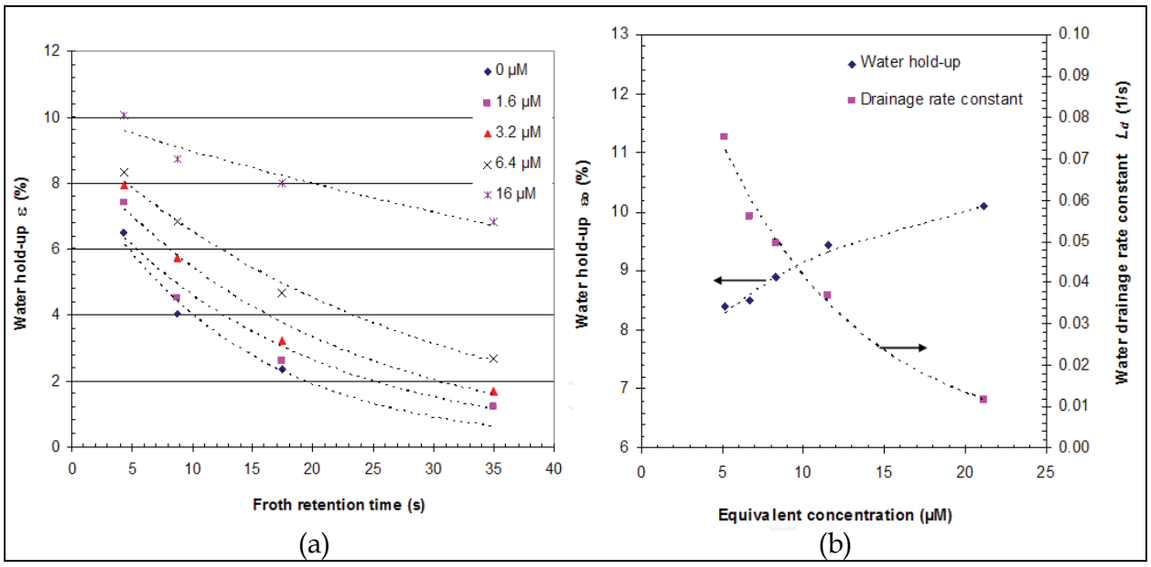

Fig. 8. Frothing behaviour of the pulp slurry in the flotation cell. (a) Water hold-up in the froth plotted as a function of the froth retention time and of the added non-ionic surfactant concentration. Dotted lines represent data fitting with Eq. 7. (b) Water hold-up at the froth/pulp slurry interface and water drainage rate constant.

4.3 Ink removal

In the absence of surfactant, ink particles are efficiently removed during flotation (Fig. 9a). However, ink removal is strongly affected by the low frothing behaviour of the pulp slurry

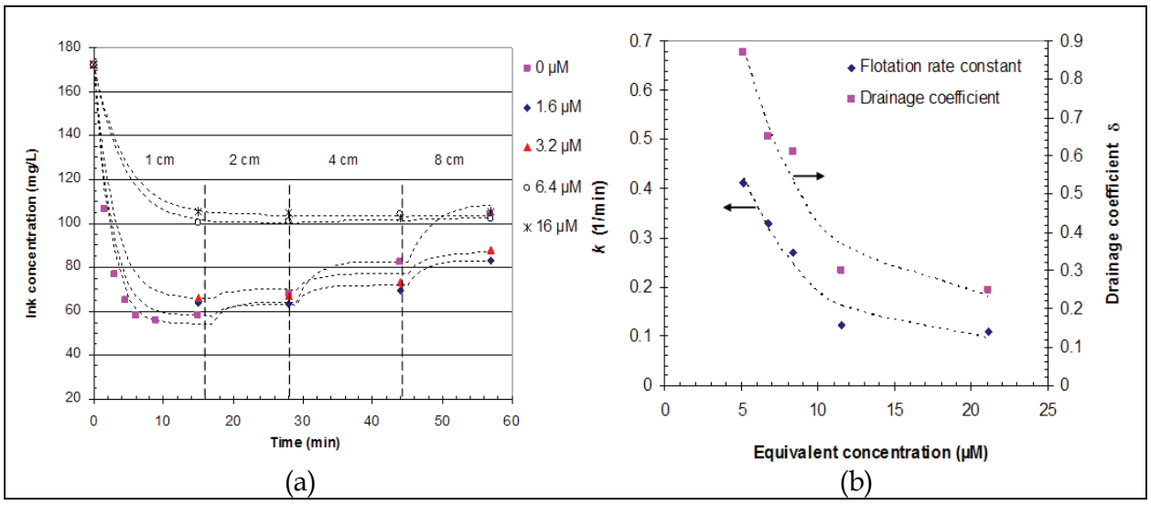

Fig. 9. Effect of surfactant concentration on ink removal. (a) Variation of ink concentration in the pulp after flotation. (b) Ink flotation rate constant and drainage coefficient.

(Fig. 8) and the increase in the froth removal thickness is responsible for a strong increase in the residual ink concentration in the floated pulp. The addition of surfactant (NP 20EO) in the pulp slurry reduces the ink flotation rate constant (Fig. 9.b) and ink removal sensitivity to the FRT. For the highest surfactant concentration, 16 µM, the ink concentration is not affected by the froth removal thickness thus reflecting the stabilization of froth bubbles. The decrease of the ink flotation rate constant for increasing NP 20EO concentration is due to non-ionic surfactant adsorption at both the bubble/ and ink/water interface which induces a decrease in both bubble surface tension and ink/water interfacial energy (Epple et al, 1994). In the froth phase, the non-ionic surfactant improves bubble stability and water hold-up reducing ink particles detachment due to bubble burst and their drainage from the froth into the aerated pulp slurry (Fig. 9b).

4.4 Fibre removal

The transfer of hydrophilic cellulose fibres in the froth decreases when increasing the surfactant concentration (Fig. 10a). As obtained for surfactant and ink, the froth stabilization due to NP 20EO addition progressively suppresses the contribution of the froth removal thickness on fibre concentration and at the highest surfactant dosage the froth has a constant fibre concentration. The decrease in the fibre entrainment coefficient shown in Fig. 10b is associated with the suppression of fibre flocculation by calcium soap and with a decrease of bubble entrapment in fibre flocs and of the convective motion of fibre/bubble flocs towards the froth.

The constant fibre drainage coefficient (Fig. 10b) indicates that fibre drainage is mainly governed by the intensity of the water drainage flow.Fillers and fine elements have a behaviour similar to that of ink particles, i.e. the increase in surfactant dosage depressed fillers/fines flotation and drainage.

5. Simulation of conventional flotation deinking banks

5.1 Implementation of model equations in a process simulation software

Within the current industrial context (environmental and safety constraints, globalization of the economy, need to shorten the "time to market" of products), computer science is more

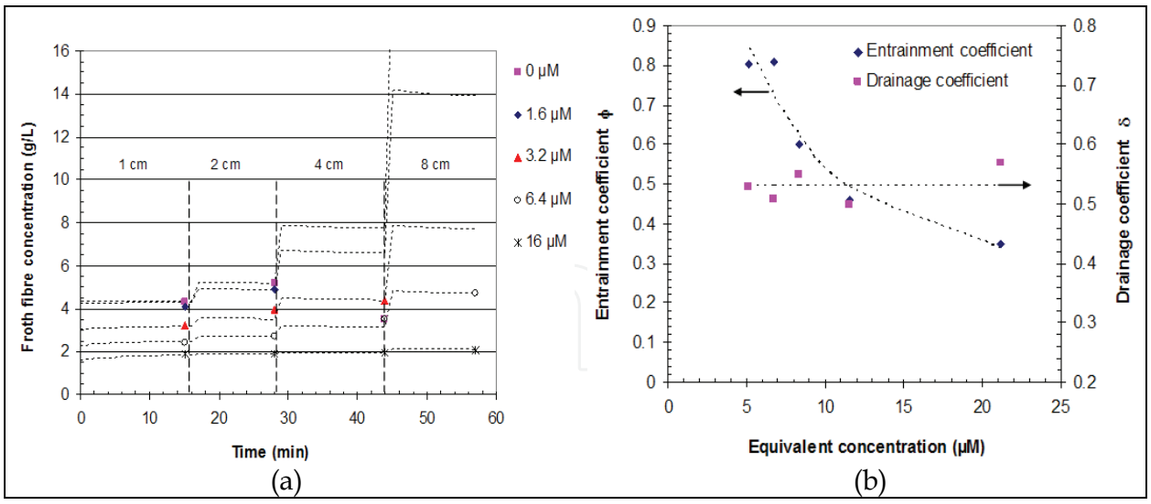

Fig. 10. Fibre removal in the froth. (a) Influence of froth removal height and surfactant concentration on the fibre concentration in the froth during flotation. (b) Fibre entrainment and drainage coefficients plotted as a function of surfactant concentration.

and more often used to design, analyse and optimize industrial processes. This specific area, called "Computer Aided Process Engineering" (CAPE), knows a big success in industries such as oil and gas, chemical and pharmaceutical. Process simulation software are used by chemical engineers in order to provide them with material and energy balances of the process, physical properties of the streams and elements required for equipment design, such as heat duty of exchangers or columns hydraulics. Moreover, process simulation software can also be used for cost estimates (capital expenditure, CAPEX and operational expense, OPEX), to evaluate environmental or security impact, to optimize flowsheets or operating conditions, for debottlenecking of an existing plant, for operator training… At a conceptual level, two kinds of process simulation software exist, the "module oriented" and the "equation oriented" approaches. Software based on this last approach are mainly dedicated to process dynamic simulation (Aspen Dynamics, gPROMS) and they can be compared to solvers for systems of algebraic and differential equations, directly written by users. The "module oriented" approach is adopted by most of the commercial process simulation software (Aspen Plus, Chemcad, Pro/II, ProSimPlus) and correspond to the natural conception of a process, which is constituted by unit operations dedicated to a specific task (heat transfer, reaction, separation). A general view of the structure of these software is provided on Fig. 11.

These software provide unit operation library, including most common units such as chemical reactors, heat exchangers, distillation or absorption columns, pumps, turbines, compressors and, sometimes, some more specific equipments such as brazed plate fin heat exchangers, belt filters.

User supplies operating and sizing parameters of each unit operations (also called modules) and linked them with streams, which represent material, energy or information flux circulating between the equipments of the real process. Other important parts of a process simulation software are the databases and the physical properties server, on which rely unit operations models to give consistent results, and solvers, which are numerical tools required to access convergence of the full flow sheet.

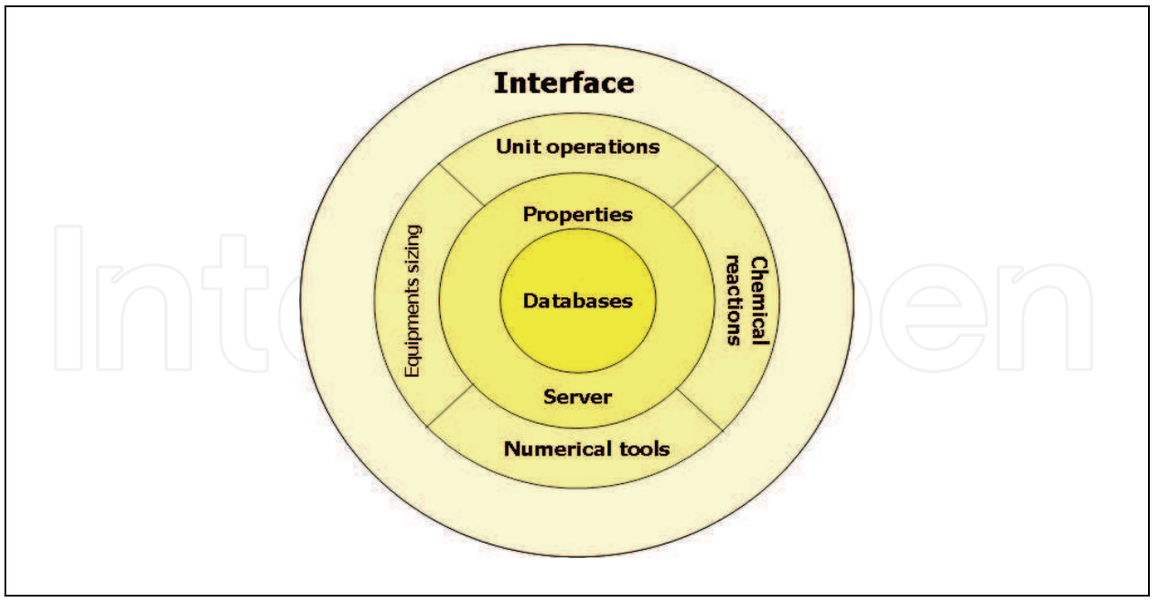

Fig. 11. Structure of a process simulation software.

Pure component databases include fixed-value properties (molar weight, critical point characteristics, normal boiling point…) and correlation coefficients for temperature-dependent properties (liquid and vapour heat capacity, vapour pressure, liquid and vapour viscosity…). The main reference for thermophysical properties of pure components is DIPPR (Design Institute for Physical Property Data, http://dippr.byu.edu/) which includes, in its 2008 version, 49 thermophysical properties (34 constant properties and 15 temperature-dependent properties) for 1973 compounds. This number of compounds is to compare with the number of chemical substances referenced by the Chemical Abstracts (http://www.cas.org/), which was greater than 33 millions in 2008. The difference between these two figures shows the importance to have models to predict pure physical properties. These models can be based on chemical structure or intrinsic properties of the molecule (molar weight, normal boiling point, critical temperature…), but they are then mainly reliable for a given chemical family. The use of molecular simulation becomes more and more frequent to compute missing data.

Modelling of a physical system rests on the knowledge of pure component and binary properties. Thus, binary interaction parameters between compounds are generally required by thermodynamic models to obtain the mixture behaviour. These parameters are obtained by fitting experimental data to thermodynamics model, the main sources of these data being the DECHEMA (http://www.dechema.de/en/start_en.html) and the NIST (http://www.nist.gov/index.html). Two kinds of methods exist in order to compute fluid phase equilibria. The first way to solve the problem consists in applying a different model to each phase: fugacities in liquid phase are calculated from a reference state which is characterized by the pure component in the same conditions of physical state, temperature and pressure, ideal laws being corrected by using a Gibbs free energy model or an activity coefficients model (NRTL, UNIQUAC, UNIFAC…). Fugacities in vapor phase are calculated by using an Equation of State (ideal gases, SRK, PR…). These methods are used in order to represent the heterogeneity of the system and are classically called heterogeneous methods. Their use covers the low pressure field and it should be noted that they do not satisfy the

continuity in the critical zone between vapour phase and liquid phase. The second way to solve the fluid phase equilibria calculation consists in homogeneous methods, which apply the same model, usually an Equation of State, to the two phases, allowing thus to ensure continuity at the critical point. Equations of State with their classical mixing rules (SRK, PR, LKP…) are included in this second category. However, the field of application of these model is limited to non polar or few polar systems. By integrating Gibbs free energy models in the mixing rules for Cubic Equations of State, some authors succeeded in merging both approaches. These models are often called combined approach. It has to be noted that some specific models have been developed for some particular fields of application, like electrolyte solutions, strong acids…

User interface helps users to transcribe its problem in the process simulation software language. Providers now propose graphical tools which allows user to build his flowsheet by "drag-and-drop". Numerous tools are also available to ensure fast access to information and convenient learning: information layers, colour management, right click, double click...

New communication standard, called CAPE-OPEN (http://www.colan.org/), is developed to permit the interoperability and integration of software components in process simulation software. Thanks to this standard, a commercial process simulation software can now use a unit operation or a thermodynamic model developed by an expert. With this approach, a process simulation software becomes a blend of software components focused on the real needs expressed by the user.

Within this context, correlations shown in Figs. 6-10 and Eqs. (1-7) were coded in FORTRAN in order to obtain a module for the flotation deinking unit operation. The effect of non-ionic surfactant concentration and distribution on ink removal selectivity was then simulated for the conventional multistage flotation system shown in Fig. 12.

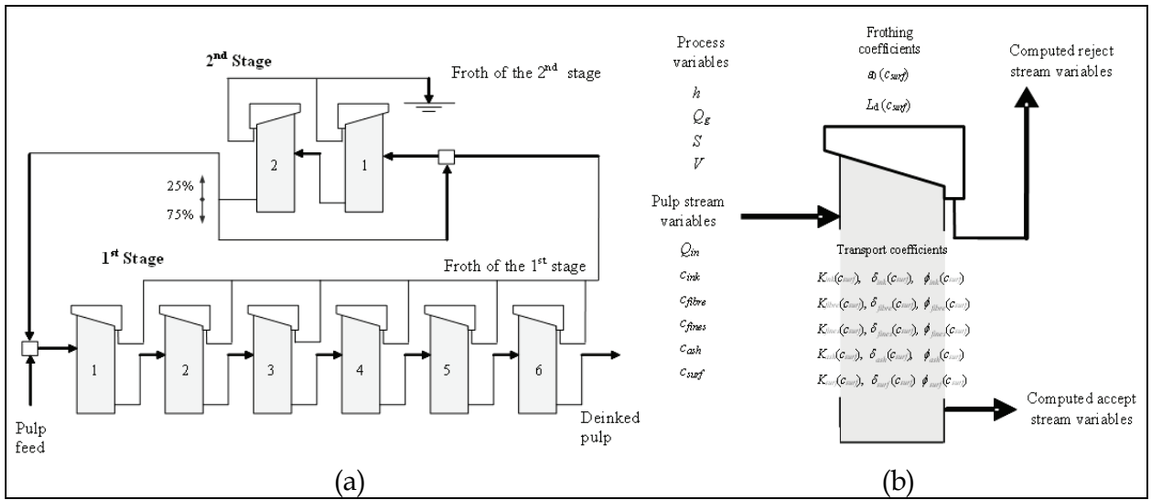

Fig. 12. Scheme of the conventional multistage deinking line simulated in this study (a) and of relevant pulp stream, flotation process and particle transport variables used to simulate each flotation unit (b).

In the simulated system (Fig. 12), a pulp stream of 32000 L/min is processed in a first stage composed by six flotation cells in series. The outlet pulp of the sixth cell is considered as the outlet of the entire system, whereas, froths generated in the first stage are mixed and further processed in a second stage made of a series of two flotation cells. The froth of the second

stage is the reject of the entire system. In order to insure a froth flow sufficient to feed the second stage and to avoid ink drainage, the froth is removed from the first stage with no retention and 75% of the pulp stream processed in the second stage is circulated at the inlet of the second stage. The remaining 25% is cascaded back at the inlet of the first stage. The froth retention time in the second stage ranges between 10 s and 4 min to stabilize the water reject to 5% (i.e. 1600 L/min). Main characteristics of the flotation line used to run simulations are given in Table 2.

Overall mass balance calculations involving multi stage systems were resolved using a process simulation software (ProSimPlus). Transport coefficients in each flotation cell composing the multistage system were calculated from the surfactant concentration at the inlet of each unit.

Volume (L)	Feed flow (L/min)	Aeration rate per cell (%)	Cross section (m^2)	Feed consistency (g/L)	Line capacity (T/day)
20000	40000	50	12	10	580

Table 2. Characteristics of each flotation cell in the simulated de-inking line.

5.2 Surfactant removal

As shown in Fig. 13a, for a constant surfactant concentration in the pulp feed flow, the surfactant load progressively decreases when the pulp is processed all along the first and the second stage. However, within the range of simulated conditions, the surfactant concentration in the second stage is ~1.5 times higher than in the first stage indicating the low capacity of the first line to concentrate surfactants in the froth phase. Surfactant removal efficiencies illustrated in Fig. 13b show that flotation units in the first stage have similar yield which asymptotically increases from ~6% to ~15%. This trend can be associated to the influence of surfactant concentration on the flotation rate and on pulp frothing. With a low

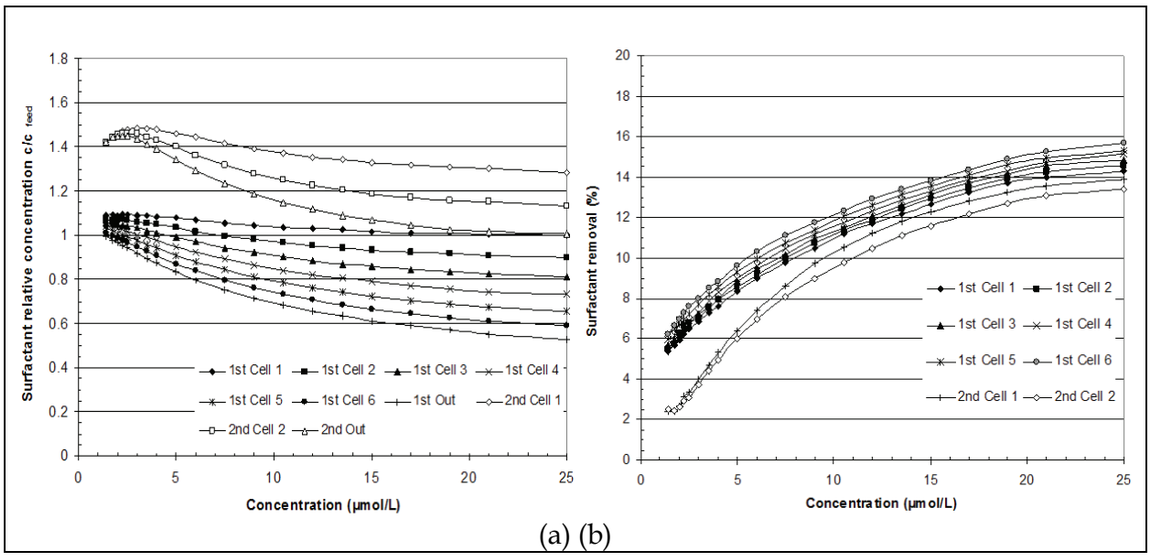

(a) (b)

Fig. 13. Effect of surfactant concentration in the pulp feed flow on surfactant distribution and removal. Surfactant concentration (a) and removal (b) in each flotation unit composing the multistage system.

surfactant concentration in the feed flow, surfactant removal in flotation cells of the second stage is lower than in the first stage. Similar yields are obtained with extremely high surfactant concentrations, i.e. >15 μmol/L. The different froth retention time in the first and in the second stage is at the origin of this trend. Indeed, in the first stage the froth is removed with no retention and surfactant molecules are subjected only to flotation and entrainment. Whereas, in the second stage the froth retention time ranges between 10 s and 4 min in order to promote water drainage and to stabilise the froth flow at 1600 L/min.

5.3 Ink removal

For all simulated concentrations, mixing the feed pulp with the pulp flow cascaded back from the second stage gives an increase in the ink concentration at the inlet of the first stage (Fig. 14a). In general, the ink concentration progressively decreases all along the first and the second stage, however, the ink distribution in the deinking line is strongly affected by the surfactant concentration. Fig. 14a shows that, at high surfactant load, the ink concentration along the deinking line progressively converges to the ink concentration in the feed flow. In this condition, the collision and the attachment of ink particles to air bubbles is disfavoured, flotation is depressed and ink removal is due to the hydraulic partitioning of the pulp flow into the reject and the floated pulp streams.

Ink removal versus surfactant concentration plots illustrated in Fig. 14b show that in all flotation cells of the first stage ink removal monotonically decreases, while in the second stage a peak in ink removal appears at 3 μmol/L. For all simulated conditions, ink removal in the second stage is lower than in the first stage. This behaviour is associated to different froth retention time and surfactant concentration in the two stages (Fig. 13a).

The peak in ink removal in the second stage reflected the progressive depression of ink upward transfer from the pulp to the froth by flotation and of ink drop back from the froth to the pulp by drainage. At low surfactant concentration, < 3 μmol/L, ink removal is governed by particle transport in the froth. The froth is unstable and bubble burst and water drainage induce ink to drop back into the pulp with an ensuing decrease in ink removal. At

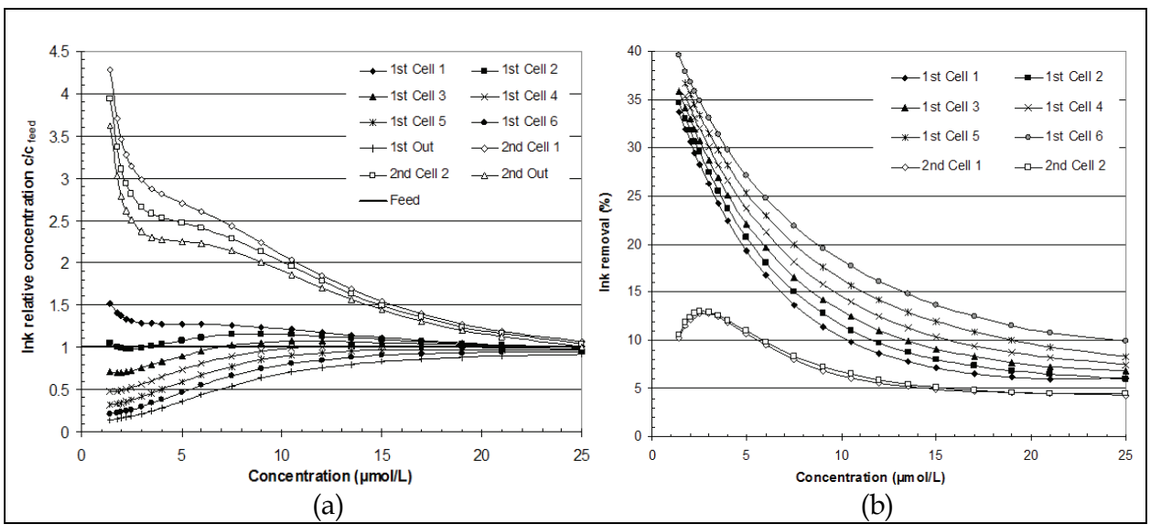

Fig. 14. Ink distribution and removal in the flotation line at increasing surfactant concentration in the pulp feed flow. (a) Ink concentration, (b) ink removal.

high surfactant concentration, > 3 µmol/L, froth bubbles are progressively stabilized and ink drainage is reduced. The presence of a maximum in the ink removal vs. surfactant concentration curve corresponds to the best compromise between froth stabilization and ink floatability depression.

5.4 Process yield

Simulation results show that both the variation of surfactant load in the pulp feed flow and its distribution in the two flotation stages affect the yield of the deinking line. Except for a peak in ink removal in the second stage at 3 µmol/L, Fig. 15a shows that the ink removal efficiency of the entire deinking line progressively decreases when increasing surfactant concentration.

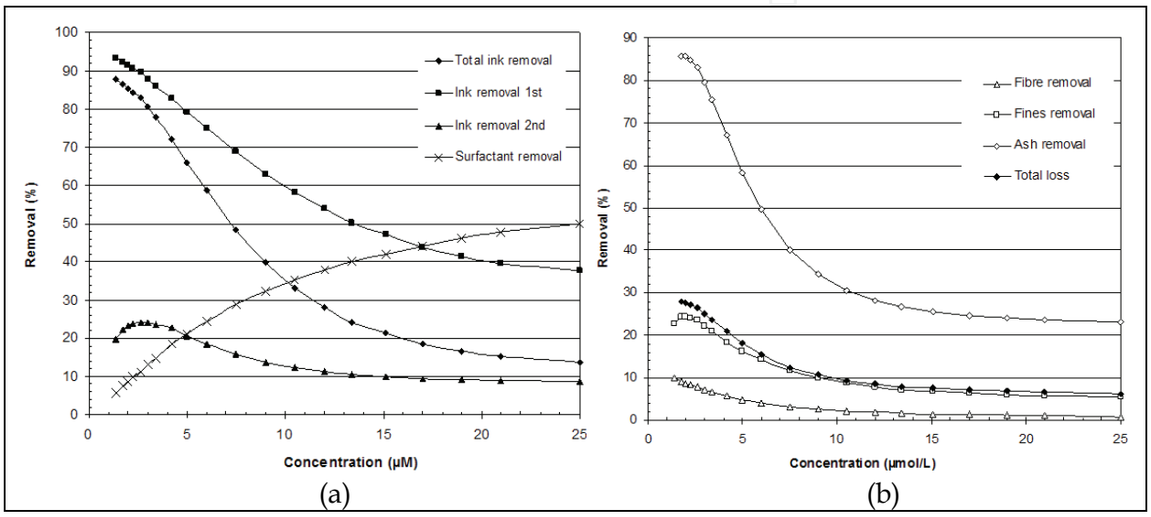

Fig. 15. Total ink and surfactant removal (a) and fibres, fines, ash loss (b) plotted as a function of surfactant concentration in the pulp feed flow.

Similar trends are obtained for fibre, fines and ash (Fig. 15b) and only surfactant removal increases when increasing the surfactant load in the pulp feed flow. Fig. 15 shows that with a surfactant load in the pulp flow comparable with the amount released by a standard pulp stock composition of 50% old newspaper and 50% old magazines, i.e. ~4 µmol/L, ink is efficiently removed (~70%), fibre, fines and ash loss have realistic values for a deinking line, i.e. 5, 19 and 65% respectively, and surfactant removal does not exceed 17%. The high sensitivity of the process yield to the surfactant load in the pulp stream and the low surfactant removal efficiency lead to assume that a conventional deinking line weakly attenuates fluctuations in the amount of surface active agents released by recovered papers with a direct effect on the stability of the process yield and on surfactant accumulation in process waters.

5.5 Comparison of simulation results with mill data

Fig. 16a shows that the residual ink content obtained by simulation with a surfactant load of 4 µmol/L is in good agreement with data collected during mill trial. In the first stage, residual ink obtained from simulation displays higher values than experimental data. This mismatch can be ascribed to the different ink load in the pulp feed flow.

The residual ink content in the floated pulp (ERIC) is lower than that of the model pulp used in laboratory experiments and to run simulations (i.e. 830 ppm). When using the industrial pulp composition to run simulations this discrepancy is strongly attenuated.
The variation of the surfactant concentration in the deinking mill is in good agreement with simulation results. Fig. 16b shows that surfactant concentration in the first stage is nearly constant and the decrease predicted by process simulation can not be observed since it is within the experimental error. As predicted by the simulation, the surfactant concentration in the second stage is 1.4-1.5 times higher than in the first stage and it progressively decreases all along the line. Ink and surfactant removal determined for the industrial deinking line in the first and second stages matches with quite good accuracy with the yield predicted by process simulation (Fig. 17) thus indicating that particle and water transport mechanisms used for the simulation of the industrial line describe with reasonable accuracy the deinking process.

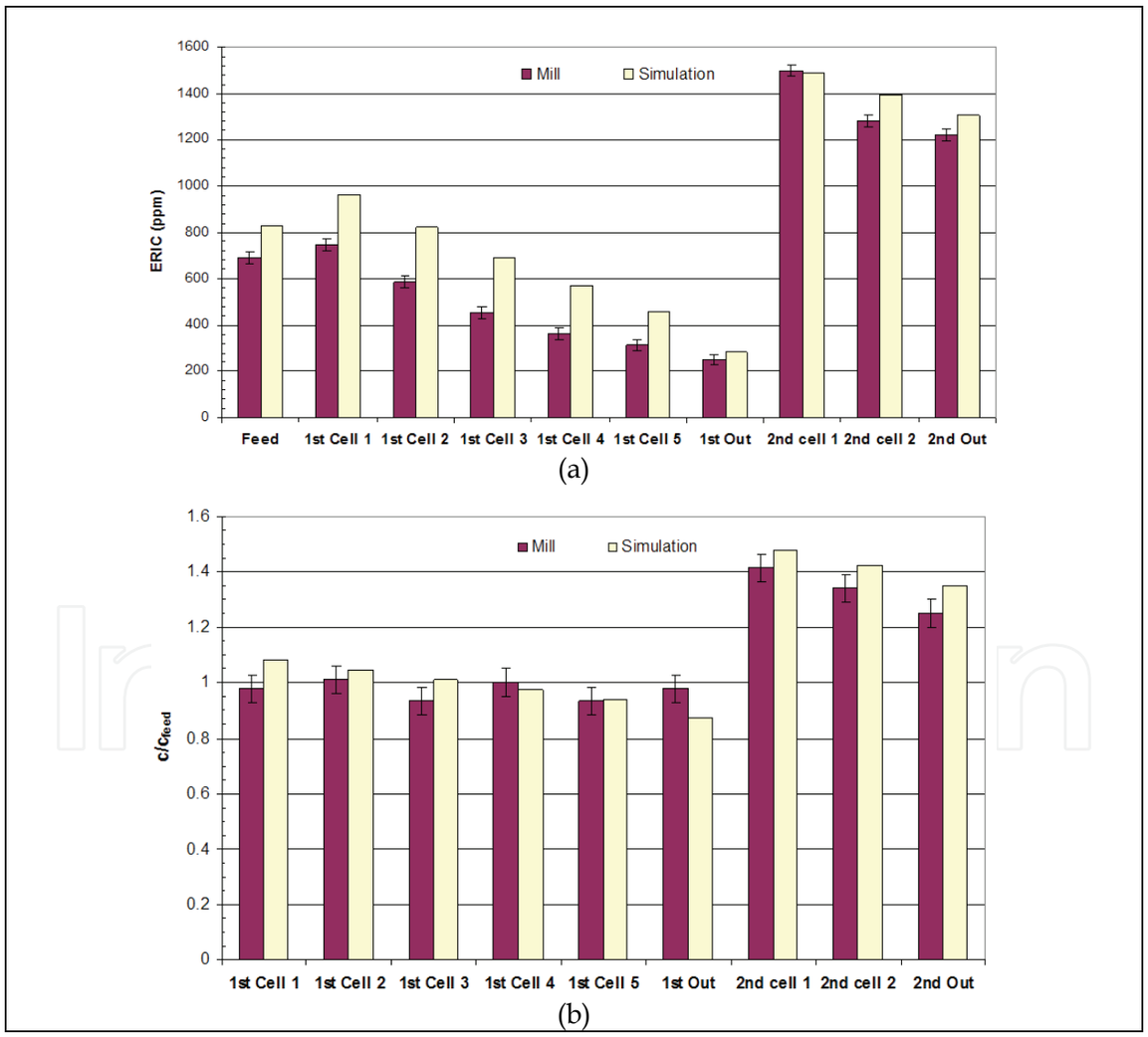

Fig. 16. Comparison of residual ink concentration (a) and surfactant relative concentration (b) obtained from process simulation with mill data.

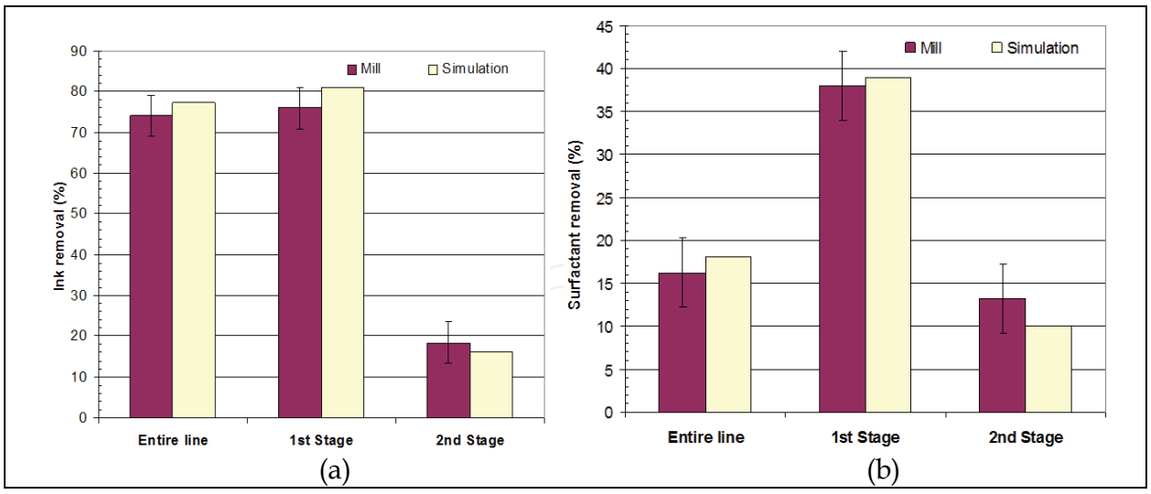

Fig. 17. Comparison of ink (a) and surfactant removal (b) obtained at the industrial scale with simulation results.

6. Optimization of deinking lines by process simulation

6.1 Deinking line layout

In order to clarify the contribution of multistage deinking lines design on ink removal and process yield, six bank configurations of increasing complexity are modelled. As summarized in Table 3, flotation banks are assembled using flotation cells with two different aspect ratios, 0.7 for the tank cell, 2 for the column cell, and with a constant pulp capacity of 20 m^3. With both cell geometries, pulp aeration is assumed to take place in Venturi aerators with an aeration rate Q_g/Q_{pulp} = 0.5 and a pressure drop of 1.2 bar (Kemper, 1999). To run simulations under realistic conditions, the superficial gas velocity in a single column cell is set at 2.4 cm/s, which corresponds to an air flow rate of 10 m^3/min or half that in the tank cell. Similarly, the pulp flow processed in flotation columns is limited to a maximal value of 10 m^3/min. Fig. 18a-d illustrates the four single-stage lines simulated in this study. The first case (Fig. 18a), consists in a simple series of flotation tanks, with common launder collecting flotation froths from each cell to produce the line reject. The number of tanks is varied from 6 to 9. In order to limit fibre loss, rejects of flotation cells at the end of the line are cascaded back at the line inlet (Fig. 18b) while the froth rejected from the first few cells is rejected. Using this configuration, the simulation is carried out with the number of tanks in the line and cascaded reject flows being used as main variables. In the third configuration (Fig. 18c), the pulp retention time at the head of the line is doubled by placing two tanks in parallel followed by a series of 7 tanks whose rejects are returned at the line inlet. The last single-stage configuration (Fig. 18d) consists in a stack of 4 to 6 flotation columns in parallel, followed by a series of 3 to 5 tanks whose rejects are sent back to the line inlet. The aim of this configuration is to increase ink concentration and pulp retention time at the head of the line and to assess the potential of column flotation for ink removal efficiency.

As depicted in Fig. 18, two- and three-stage deinking lines were also simulated. As previously mentioned, the two-stage line shown in Fig. 18e is the most widely used one in flotation deinking. In this classical configuration, reject of the first stage, are generated in 5 to 9 primary cells in series. To recover valuable fibres in these combined reject stream, rejects of the primary line are processed in a second stage with 1 to 4 tanks. The number of flotation

tanks in the first and in the second stage is here used as main variable to optimize the line design. The three-stage line shown in Fig. 18f is made of a first stage with 7 to 8 flotation tanks, a second stage with 2 tanks and a third stage with 1 tank. The pulp processed in the third stage is partitioned between the inlets of the third and of the second stage.

Pulp volume (m^3)	Cross section (m^2)	Aspect ratio h/d	Pulp feed flow (m^3/min)	Air flow (m^3/min)	Superficial gas velocity (cm/s)	Gas hold-up+ (%)	Ink flotation rate constant (1/min)	Ink removal (%)
20	12	~0.7	40	20	2.8	10-20	~0.45	20-35
20	7	~2	40/*m**	10	2.4	30-40	~0.52	50-65

Table 3. Relevant characteristics of flotation units used to assembly the flotation lines simulated in this study. + Estimated assuming a bubble slip velocity relative to the pulp downstream flow of ~7 cm/s.

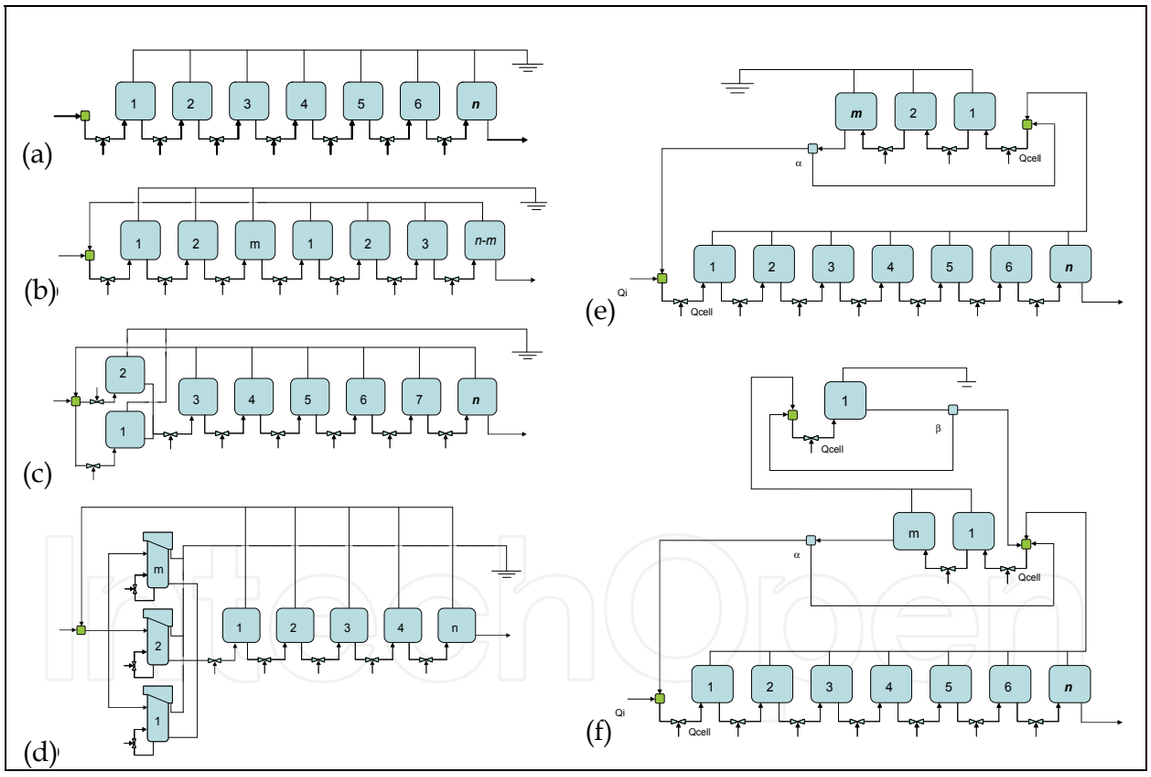

Fig. 18. Flotation lines simulated in this study. (a) Simple line made of a series of *n* flotation cells. (b) Line with *n* flotation cells with the reject of the last *n-m* cells cascaded back at the line inlet. (c) Line composed by *n* flotation cells with the first two cells in parallel and the remaining cells in series. The reject of the last *n*-2 cells is cascaded back at the inlet of the line. (d) Line composed by a stack of *m* flotation columns in parallel and a series of *n* cells. The reject of flotation cells is cascaded back at the inlet of the line. (e) Conventional two-stage line with *n* cells in the primary stage and *m* cells in the secondary stage. (f) Three-stage line with $n = 8$, $m = 2$.

The pulp processed in the second stage is partitioned between the inlets of the second stage itself and of the first stage. In order to limit the number of variables, all simulations are run with zero froth retention time. Under this condition, ink removal and fibre/fillers loss are maximized because particle and water drainage phenomena from the froth to the pulp are suppressed but this is obtained at the expense of ink removal selectivity. Simulation results are therefore representative of deinking lines operated at their maximal ink removal capacity.

6.2 Ink removal selectivity and specific energy consumption

Flotation lines assembled here for simulation purposes are characterized by a fixed (tank cells) and an adjustable (column cells) feed flow. Since the introduction of recirculation loops modifies the processing capacity and the pulp retention time in the whole line, predicting particle removal efficiencies is not sufficient to establish a performance scale between different configurations. Consequently, the specific energy consumption, which is given by the equation

$$SE = \frac{P_{inj} \cdot \sum_n Q_g}{\rho \cdot Q_{out} \cdot c_{out}} \tag{8}$$

where Q_g is the gas flow injected in each flotation cell (n) in the multistage system, P_{inj} the pressure feed of each static aerator (1.2 bar), ρ the aeration rate Q_g/Q_{pulp} (0.5 in the simulated conditions), Q_{out} and c_{out} are the pulp volumetric flow and consistency at the outlet of the deinking line, the ink removal efficiency and the ink removal selectivity (Z factor) (Zhu et al., 2005), have to be taken into account to establish a correlation between process efficiency and line design.

Fig. 19a illustrates that when the cascade ratio is raised in single-stage lines, the deinking selectivity increases by 4-5 times, whereas the specific energy consumption slightly decreases. Reduced energy is caused by a net increase in pulp production capacity. However, these gains are generally associated with a decrease in ink removal. Hence, the reference target of 80 % ink removal with selectivity factor Z = 8 could only be obtained with a line made of 9 tanks with a cascade ratio of 0.6 and a specific energy consumption of 60 kWh/t. Because target ink removal and selectivity can be achieved only by increasing energy consumption, this configuration does not represent a real gain in terms of process performance. The addition of a high ink removal efficiency stage comprising a stack of flotation columns in parallel at the line head, Fig. 19b, reduces specific energy consumption by 25-50 %. Nevertheless, the efficient removal of floatable mineral fillers and the absence of hydrophilic particle drainage in the froth limits the selectivity factor to ~7.5. According to experimental studies (Robertson et al. 1998; Zhu & Tan, 2005), the increase of the froth retention time and the implementation of a froth washing stage would improve the selectivity factor with a minimum loss in ink removal. Under these conditions, a flotation columns stack equipped with optimized froth retention/washing systems would markedly decrease specific energy consumption. Similarly to the results obtained for single-stage lines, Fig. 20a shows that improved ink removal selectivity in two-stage lines is coupled with a decrease ink removal.

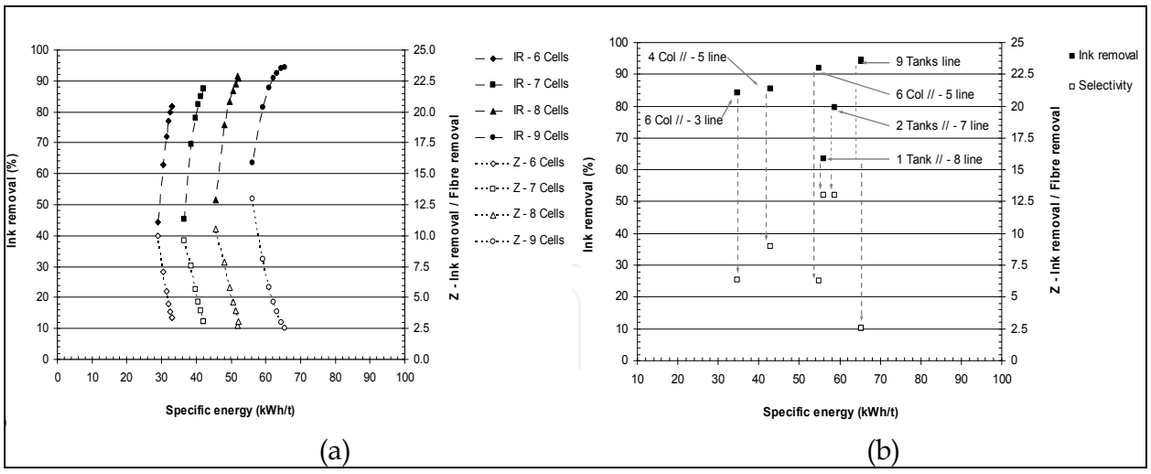

Fig. 19. Ink removal efficiency and selectivity obtained for tested configurations plotted as a function of the specific energy consumption. (a) Flotation line composed by 6 to 9 flotation cells and with the reject of the last *n-m* cells cascaded back at the line inlet (Fig. 18a-b). (b) Flotation line composed by a stack of flotation cells or columns in parallel followed by a series of flotation cells (Fig. 18c-d).

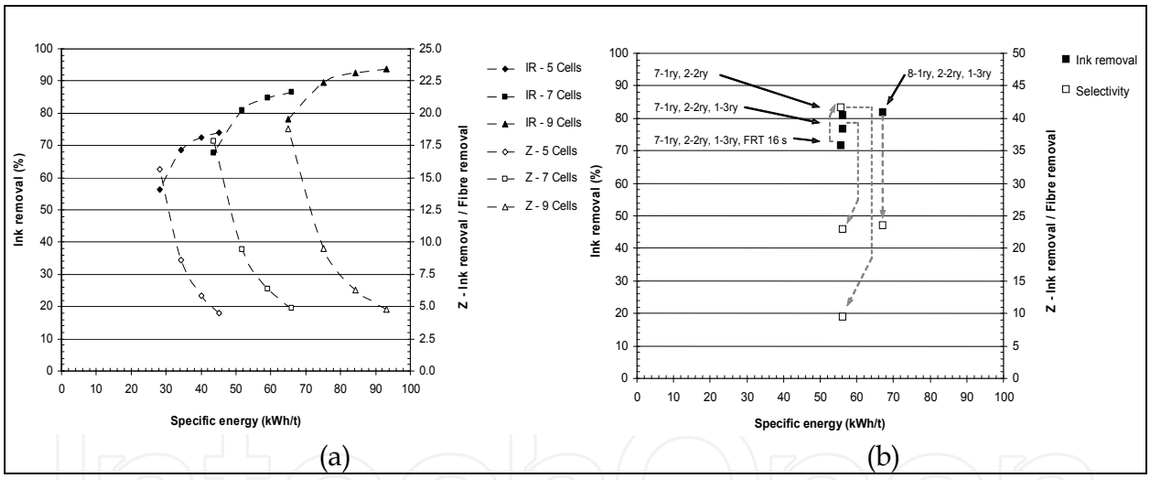

Fig. 20. Ink removal efficiency and selectivity obtained for tested configurations plotted as a function of the specific energy consumption. (a) Deinking line composed by a 1ry and a 2ry stage with different number of flotation cells in the two stages (Fig. 18e). The legend in the pictures indicates the number of cells in the 1ry stage. b) Line of 3 stages (Fig. 18f).

The selectivity factor appears to be directly correlated to the number of flotation tanks in the secondary line as it progressively decreases from ~17.5 to 5 when increasing the number of tanks in the second stage. Selectivity drops when the reject flow increases which, for two- and single-stage lines, is induced by the increase of the number of tanks in the second stage and the decrease of the cascade ratio, respectively.

In turn, ink removal efficiency is found here to be governed by the number of cells in the first stage. Fig. 20a shows that, with a constant number of tanks in the second stage, ink removal increases by 10 % for each additional cell in the first stage, while selectivity slightly

increases. Seven tanks in the first stage and two tanks in the second stage are needed to reach the target of 80 % ink removal and a selectivity factor of 9. With this configuration, the specific energy consumption of the two-stage line (52 kWh/t) is lower than the energy required by a single stage line with the same deinking efficiency/selectivity (60 kWh/t). Overall, the best energetic efficiency is given by the single line with a stack of six flotation columns at the line head (Fig. 19b).

If we consider the two-stage line with ink removal and selectivity targets as reference system, the addition of a third stage with a single tank boosts up selectivity, slightly decreases ink removal from 81 to 78% and does not affect specific energy consumption (Fig. 20b). The selectivity index of the three-stage line can be further increased from 21.5 to 41 by setting at 16 s froth residence time in the third stage cell. However, the selectivity gain is coupled to a decrease in ink removal from 78 to 72 % and the need for an additional tank in the first stage to attain the ink removal target of 80 %. With this last configuration of 8 tanks in the first stage, 2 tanks in the second stage and 1 tank in the third stage, 80 % ink removal is attained along the highest selectivity factor of all tested configurations. However, the gain in separation efficiency results in a sizeable increase in the specific energy consumption. As for the other tested configurations, the effective benefit provided by this configuration should be thoroughly evaluated in the light of recovered papers, rejects disposal and energy costs.

7. Conclusions

This chapter summarizes the four steps that have been necessary to develop and validate a process simulation module that can be used for the management of multistage flotation deinking lines, namely, i) the identification of mass transfer equations, ii) their validation on a laboratory-scale flotation cell, iii) the correlation of mass transfer coefficients with the addition of chemical additives and iv) the simulation of industrial flotation deinking banks.

Due to the variability of raw materials and the complexity of physical laws governing flotation phenomena in fibre slurries, general mass transport equations were derived from minerals flotation and validated on a laboratory flotation column when processing a recovered papers pulp slurry in the presence of increasing concentration of a model non-ionic surfactant.

Cross correlations between particle transport coefficients and surfactant concentration obtained from laboratory tests were used to simulate an industrial two-stage flotation deinking line and a good agreement between simulation and mill data was obtained thus validating the use of the present approach for process simulation.

Thereafter, the contribution of flotation deinking banks design on ink removal efficiency, selectivity and specific energy consumption was simulated in order to establish direct correlations between the line design and its performance. The simulation of a progressive increase of the line complexity from a one to a three-stage configuration and the use of tank/column cells showed that:

- In single-stage banks, ink removal selectivity and specific energy consumption can be improved by increasing the cascade ratio (i.e. the ratio between the number of cascaded cells and the total number of cells in the line) with a minimum decrease in the ink removal efficiency. Above a cascade ratio of 0.6, the ink removal efficiency drops.

- The addition of a stack of flotation columns in the head of a single stage line gives an increase in ink removal selectivity and a decrease in specific energy consumption.
- In two-stage banks, the ink removal efficiency is mainly affected by the number of flotation tanks in the first stage, whereas, the number of cells in the second stage affects the fibre removal, which linearly increases with the number of cells.
- The addition of a third stage allows increasing ink removal selectivity with a negligible effect on the ink removal efficiency and on the specific energy consumption.
- Overall, the best deinking performance is obtained with a stack of flotation columns at the line head and the three-stage bankg.

8. Acknowledgement

This paper is the outline of a research project conducted over the last four years. Authors wish to thank Mr. J. Allix, Dr. B. Carré, Dr. G. Dorris, Dr. F. Julien Saint Amand, Mr. X. Rousset and Dr. E. Zeno for their valuable contribution.

9. References

Beneventi, D.; Allix, J.; Zeno, E.; Nortier, P.; Carré, B. (2009). Simulation of surfactant contribution to ink removal selectivity in flotation deinking lines, *Sep. Purif. Technol.*, 64 (3), 357-367.

Beneventi, D.; Benesse, M.; Carré, B.; Julien Saint Amand, F.; Salgueiro, L. (2007). Modelling deinking selectivity in multistage flotation systems. *Sep. Purif. Technol.*, 54 (1), 57-67.

Beneventi, D.; Rousset, X.; Zeno, E. (2006). Modelling transport phenomena in a flotation deinking column. Focus on gas flow, pulp and froth retention time, *Int. J. Miner. Process.*, 80 (1), 43-57.

Beneventi, D.; Zeno, E.; Nortier, P.; Carré, B.; Dorris, G. (2009). Optimization and Management of Flotation Deinking Banks by Process Simulation, *Ind. Eng. Chem. Res.*, 48 (8), 3964–3972.

Blanco, A.; Dahlquist, E.; Kappen, J.; Manninen, J.; Negro, C.; Ritala, R. (2006). Modelling and simulation in pulp and paper industry. Current state and future perspectives, *Cellulose Chem. Tech.*, 40 (3-4), 249-258.

Bloom, F. (2006). A mathematical model of continuous flotation deinking, *Math. Comp. Model. Dyn. Sys.*, 12 (4), 277-311.

Bloom, F.; Heindel, T. J. (2003). Modeling flotation separation in a semi-batch process, *Chem. Eng. Sci.*, 58 (2), 353-365.

Brun, J.; Delagoutte, T.; Blanco, A. (2003). Identification and quantification of the main sources of dissolved and colloidal materials in recovered papers, *Revue ATI*, 57 (4), 12-18.

Byström, S.; Lönnstedt, L. (2000). Paper recycling: a discussion of methodological approaches, *Resour. Conserv. Recycl.*, 28 (1), 55–65.

Carré, B.; Magnin, L. (2003). Printing processes and deinkability, *International paperworld*, 12, 41-45.

Chabot, B.; Gopal, A.; Krinshnagopalan (1996). Flexographic newspaper deinking : treatment of wash filtrate effluent by membrane technology, *4th Research Forum on Recycling*, Chateau Frontenac, Quebec, October 7-9, 233-242.

Chaiarrekij, S.; Dhingra, H.; Ramarao, B. V. (2000). Deinking of recycled pulps using column flotation: energy and environmental benefits, *Resour. Conserv. Recycl.*, 28 (3-4), 219-226.

Cho, B.U.; Ryu, J.Y.; Song, B.K. (2009). Modeling and simulation of separation process in flotation system, *J. Ind. Eng. Chem.*, 15 (2), 196-201.

Comley, B.A.; Harris, P.J.; Bradshaw, D.J.; Harris, M.C. (2002). Frother characterization using dynamic surface tension measurements, *Int. J. Mineral Process.*, 64, 81-100.

Dahlquist, E. (2008). Process Simulation for Pulp and Paper Industries: Current Practice and Future Trend, Chem. Prod. Process Modeling, 3 (1), 18.

Danov, K.D.; Valkovska, D.S.; Ivanov, I.B. (1999). Effect of Surfactants on the Film Drainage, *J. Colloid Int. Sci.*, 211, 291-303.

Dorris, G. M.; Nguyen, N. (1995). Flotation of model inks. Part II. Flexo ink dispersions without fibres, *J. Pulp Paper Sci.*, 21 (2), 55-62.

Dreyer, A.; Britz, H.; Renner, K.; Heikkilä, P.; Grimm, M. (2008). Circuit designs for secondary accept in deinking flotation. *Proceedings of the 13th PTS-CTP Deinking Symposyum*, 16, 15-17 April 2008, Leipzig, Germany.

Epple, M.; Schmidt, D.C.; Berg, J.C. (1994). The effect of froth stability and wettability on the flotation of a xerographic toner, *Colloid Polym. Sci.*, 272, 1264-1272.

Gorain, B.K.; Harris, M.C.; Franzidis, J.-P.; Manlapig, E.V. (1998). The effect of froth residence time on the kinetics of flotation, *Miner. Eng.*, 11, 627-638.

Hernandez, H., Gomez, C. O.; Finch, J. (2003). A. Gas dispersion and de-inking in a flotation column, *Miner. Eng.*, 16 (8), 739-744.

Hunter, N. (2007). Fuel plus from the forest: a short review and introduction to the biorefinery concept, *Appita J.*, 60 (1), 10-12.

Johansson, B.; Strom, G. (1998). Surface chemistry of flotation deinking: effect of various chemical conditions on ink agglomerate character and floatability, *Nord. Pulp Pap. Res. J.*, 13 (1), 37-49.

Jordan, B.D.; Popson, S.J. (1994). Measuring the concentration of residual ink in recycled newsprint, *J. Pulp Paper Sci.*, 20 (6), 161-167.

Julien Saint Amand, F. (1999). Hydrodynamics of deinking flotation, *Int. J. Mineral Process.*, 56 (1), 277-316.

Kemper, M. (1999). State-of-the-art and new technologies in flotation deinking, *Int. J. Mineral Process.*, 56 (1), 317-333.

Labidi, J.; Pelach, M. A.; Turon, X.; Mutjé, P. (2007). Predicting flotation efficiency using neural networks, *Chem. Eng. Process.*, 46 (4), 314-322.

Maachar, A.; Dobby, G.S. (1992). Measurement of feed water recovery and entrainment solids recovery in flotation columns, *Canadian Metallurgical Quarterly* 31, 167-172.

Miranda, R.; Blanco, A.; Negro, C. (2009). Accumulation of dissolved and colloidal material in papermaking-Application to simulation, *Chem. Eng. J.*, 148 (2), 385-393.

Neethling, S.J.; Cilliers, J.J. (2002). Solids motion in flowing froths. *Chem. Eng. Sci.*, 57, 607-615.

Nguyen, A.V.; Harvey, P.A.; Jameson, G.J. (2003). Influence of gas flow rate and frothers on water recovery in a froth column, Miner. Eng., 16, 1143-1147.

Pirttinen, E.; Stenius, P. (1998). The effect of dissolved and colloidal substances on flotation deinking efficiency, *Progr. Paper Recycl.*, 7, 38-46.

Pugh, R.J. (2001). Dynamic Surface tension measurements in mineral flotation and de-inking flotation systems and the development of the on line dynamic surface tension detector, *Miner. Eng.*, 14, 1019-1031.

Robertson, N.; Patton, M.; Pelton, R. (1998). Washing the fibers from foams for higher yields in flotation deinking. *Tappi J.*, 81 (6), 138–142.

Ruiz, J.; Ottenio, P.; Carré, B. (2003). La simulation numérique au service des papetiers, ATIP, 57 (3), 24-31.

Schwarz, S.; Grano, S. (2005). Effect of particle hydrophobicity on particle and water transport across a flotation froth, *Colloids and Surfaces A: Physicochem. Eng. Aspects*, 256, 157-164.

Shi, F.N.; Zheng, X.F. (2003). The rheology of flotation froths, *Int. J. Miner. Process.*, 69, 115-128.

Sjoede, A.; Alriksson, B.; Joensson, L. J.; Nilvebrant, N.-O. (2007). The potential in bioethanol production from waste fiber sludges in pulp mill-based biorefineries, *Appl. Biochem. Biotech.*, 137-140 (1-12), 327-337.

Tatzer, P.; Wolf, M.; Panner, T. (2005). Industrial application for inline material sorting using hyperspectral imaging in the NIR range, *Real-Time Imaging*, 11 (2), 99-107.

Theander, K.; Pugh, R.J. (2004). Surface chemicals concepts of flotation de-inking, *Colloids and Surfaces A: Physicochem. Eng. Aspects*, 240 (1-3), 111-130.

Valkovska, D. S.; Danov, K. D.; Ivanov, I. B. (2000). Effect of surfactants on the stability of films between two colliding small bubbles, *Colloids and Surfaces A: Physicochem. Eng. Aspects*, 175, 179-192.

Vera, M.A.; Mathe, Z.T.; Franzidis, J.-P.; Harris, M.C.; Manlapig, E.V.; O'Connor, C.T. (2002). The modelling of froth zone recovery in batch and continuously operated laboratory flotation cells, *Int. J. Miner. Process.*, 64, 135-151.

Volmer, M. (1925). Thermodynamic deductions from the equation of state for adsorbed material, *J. Phys. Chem.*, 115, 233-238.

Ward, A.F.H.; Tordai, L. (1946). Time dependence of boundary tensions of solutions. I. The role of diffusion in time effects, *J. Chem. Phys.*, 14, 453-461.

Zheng, X.; Franzidis, J.-P.; Johnson, N.W. (2006). An evaluation of different models of water recovery in flotation, *Miner. Eng.*, 19, 871-882.

Zheng, X.; Franzidis, J.-P.; Johnson, N.W.; Manlapig, E.V. (2005). Modelling of entrainment in industrial flotation cells: the effect of solids suspension, *Miner. Eng.*, 18, 51-58.

Zhu, J. Y.; Tan, F. (2005). Dynamic drainage of froth with wood fibres, *Ind. Eng. Chem. Res.*, 44 (9), 3336-3342

Zhu, J.Y.; Tan, F.; Scallon, K.L.; Zhao, Y.L.; Deng, Y. (2005). Deinking selectivity (*Z*-factor): a new parameter to evaluate the performance of flotation deinking process, *Sep. Purif. Technol.*, 43 (1), 33-41.

Process Management

Edited by Maria Pomffyova

ISBN 978-953-307-085-8

Hard cover, 338 pages

Publisher InTech

Published online 01, April, 2010

Published in print edition April, 2010

The content of the book has been structured into four technical research sections with total of 18 chapters written by well recognized researchers worldwide. These sections are: 1. process and performance management and their measurement methods, 2. management of manufacturing processes with the aim to be quickly adaptable after real situation demands and their control, 3. quality management information and communication systems, their integration and risk management, 4. management processes of healthcare and water, construction and demolition waste problems and integration of environmental processes into management decisions.

How to reference

In order to correctly reference this scholarly work, feel free to copy and paste the following:

Davide Beneventi, Olivier Baudouin and Patrice Nortier (2010). Semi-Empirical Modelling and Management of Flotation Deinking Banks by Process Simulation, Process Management, Maria Pomffyova (Ed.), ISBN: 978-953-307-085-8, InTech, Available from: http://www.intechopen.com/books/process-management/semi-empirical-modelling-and-management-of-flotation-deinking-banks-by-process-simulation

INTECH
open science | open minds

InTech Europe
University Campus STeP Ri
Slavka Krautzeka 83/A
51000 Rijeka, Croatia
Phone: +385 (51) 770 447
Fax: +385 (51) 686 166
www.intechopen.com

InTech China
Unit 405, Office Block, Hotel Equatorial Shanghai
No.65, Yan An Road (West), Shanghai, 200040, China
中国上海市延安西路65号上海国际贵都大饭店办公楼405单元
Phone: +86-21-62489820
Fax: +86-21-62489821

IntechOpen